A study using waveform simulations on the applicability of seafloor strong motion records to the source process analysis

*Hisahiko Kubo[1], Shunsuke Takemura[1], Wataru Suzuki[1], Takashi Kunugi[1], Shin Aoi[1]

1. National Research Institute for Earth Science and Disaster Prevention

Because of the recent development of seafloor strong motion observation networks in the subduction zone of Japan such as DONET and S-net, seafloor strong motion records become available in the source process analysis. The use of seafloor records leads to the improvement in station coverage of the source process analysis for offshore earthquakes, which can improve the resolution and reliability of the analysis (e.g. Iida et al. 1988; Iida 1990). However, because of a limited knowledge on the offshore subsurface velocity structure, it is difficult to obtain Green's functions that can reproduce observed waveforms. Moreover, 1D synthetic waveforms, which are calculated with a 1D velocity structure model and widely used in conventional source-process analyses, are inappropriate to consider the offshore heterogeneous structure including a seawater, a rolling seafloor, thick sediments, and a subducting oceanic plate. One approach for this is to use 3D synthetic waveforms, which are calculated by 3D numerical simulations with a 3D velocity structure model; however the use of them is not easy because of a limited knowledge on the offshore structure and the high calculation cost. In this study, based on waveform simulations, we investigate the applicability of seafloor records to the source process analysis.

We prepare 3D synthetic waveforms for models with/without a seawater and 1D synthetic waveforms at S-net stations off Fukushima for near-coast and near-trench shallow crustal earthquakes in three period bands of 5-10 s, 10-25 s, and 25-50 s. 3D synthetic waveforms for a model with a seawater are calculated with a 3D FDM simulation (Takemura et al. 2015) assuming a 3D velocity structure model, which is based on the 3D subsurface structure model of J-SHIS (Fujiwara et al. 2009, 2012) including topographies and a seawater layer. 3D synthetic waveforms for a model without a seawater are calculated assuming a 3D velocity structure model, which is same as the above model but a seawater layer is replaced with an air. 1D synthetic waveforms are calculated at each station with the discrete wavenumber method (Bouchon 1981) and the reflection/transmission matrix method (Kennett and Kerry 1979) assuming a 1D velocity structure model for each station, which is extracted from the J-SHIS model.

To investigate the effect of a seawater layer, we compare the 3D synthetic waveforms for models with/without a seawater. Although the waveforms at transverse component are almost similar, the difference between their waveforms at radial and vertical components appears at periods lower than 25 s. The distribution of stations with the waveform difference depends on the horizontal event location: the waveform differences in the near-coast event are found at stations with a deep water depth, while these in the near-trench event are shown at almost all stations. Previous studies (e.g. Nakamura et al. 2014; Noguchi et al. 2016) demonstrated that the presence of a seawater and sediments leads to the excitation of oceanic Raleigh waves and that the predominant period of the fundamental mode of the Rayleigh waves depends on the seawater thickness. Our result and previous studies suggest that in the case of the near-trench earthquakes and/or the use of waveforms at stations with a deep seawater depth, appropriate waveform components and period band for the source process analysis are limited as long as Green's functions for a model without a seawater are used.

We also investigate how the 1D synthetic waveforms can reproduce the 3D synthetic waveforms considering the offshore heterogeneous structure. The waveform comparison suggests that although the amplitude difference and the time shift of S-wave and later phases are shown at many stations, there are stations that the phases of S-wave are similar. This suggests the possibility that seafloor records after the corrections of time shifts and amplitude differences can be used in the source process analysis.

Keywords: Seafloor strong motion records, Source process analysis, Waveform simulations

Source process of the October 21, 2016, Tottori-chubu earthquake

*Kazuhito Hikima[1]

1. Tokyo Electric Power Company Holdings, Inc.

<INTRODUCTION>
An M 6.6 earthquake occurred at 14:07 on October 21, 2016 in central Tottori Prefecture. During this earthquake, high acceleration records were observed within the source region. For example, JMA intensity 6- was recorded at TTR005 (K-NET, Kurayoshi), and the PGA at this station was about 1380 gal in EW component and 1490 gal in the synthetic of three components. The effect of surface geology is regarded as one of the reasons for these strong motions in general. However, two distinct wave packets are recognized in the observed waveforms in the near source region, and long period pulse like shape is dominant in the former packet, on the other hand, short period component is significant in latter packet. These observations suggest that the effects of the source process are not negligible for the strong motions. So a waveform inversion analysis was applied for this earthquake to consider the effect of the source process.

<OUTLINE of ANALYSIS>
We used the waveforms from 16 KiK-net borehole stations (by NIED) to reduce the effects of the surface geology. In Addition, two K-NET stations, TTR005 which is located immediately above the source region, and OKY015 which is located in the south of the source, were incorporated in the inversion analysis. The acceleration waveforms were filtered between 0.03 and 0.8 Hz, and were integrated to velocity waveforms for the inversion analyses.
The source processes were inverted by the multi time window analysis (Yoshida et al., 1996, Hikima, 2012). The Green’ s functions were calculated using 1-D velocity models, which were tuned by the waveform inversion method (Hikima and Koketsu, 2005), using the records of the Mw 4.1 event occurred on October 21. The fault planes of the initial models were configured by referring to the F-net mechanism solutions and the JMA hypocenter parameters. The final model was determined by considering the degree of fitness between the observed and synthetic waveforms. The size of subfaults for the inversion analyses were set in 2 km for preliminary trials, and in 1 km for the final result.

<RESULT>
The fault parameters were set tentatively as follows: the strike and the dip are 341 and 89 degree, and the length and the width are about 14 and 14 km, respectively. The depth of hypocenter is 10.6 km.
Left-lateral slip component is dominant, and the estimated moment magnitude (Mw) is about 6.2. A large slip area (asperity) was estimated around the hypocenter and its shallow part, in which the maximum slip was nearly 1.2 m. The rupture propagated toward the northern portion mainly, additionally a small asperity was estimated near the northern edge of the fault plane.

<DISCUSSION>
According to the inversion result, two asperities are obtained near the hypocenter and at the northern edge of the fault. So, it is considered plausible that these asperities are corresponding to the two wave packets observed in the waveforms. Furthermore, the larger asperity is existing between the hypocenter and the TTR005, so, the directivity effect from the asperity seems to be one of the reasons that caused the long period pulse waveform at the station. On the other hand, the short period component of the latter wave packet is the effect from the northern asperity, those slip velocity was comparatively large. Thus, it seems that the spatiotemporal source process obtained by the waveform inversion can explain the dominant characteristics of the observed waveforms.
We also calculated the stress change from the final slip distribution by using Okada's program. The stress

drop is at most 20 MPa, so, this value is comparable level with the past crustal earthquakes. This result indicates that the strong motion excitation of this earthquake was almost average level of other crustal earthquakes.

Keywords: Source process, Strong motion, Tottori-Chubu earthquake, Crustal earthquake

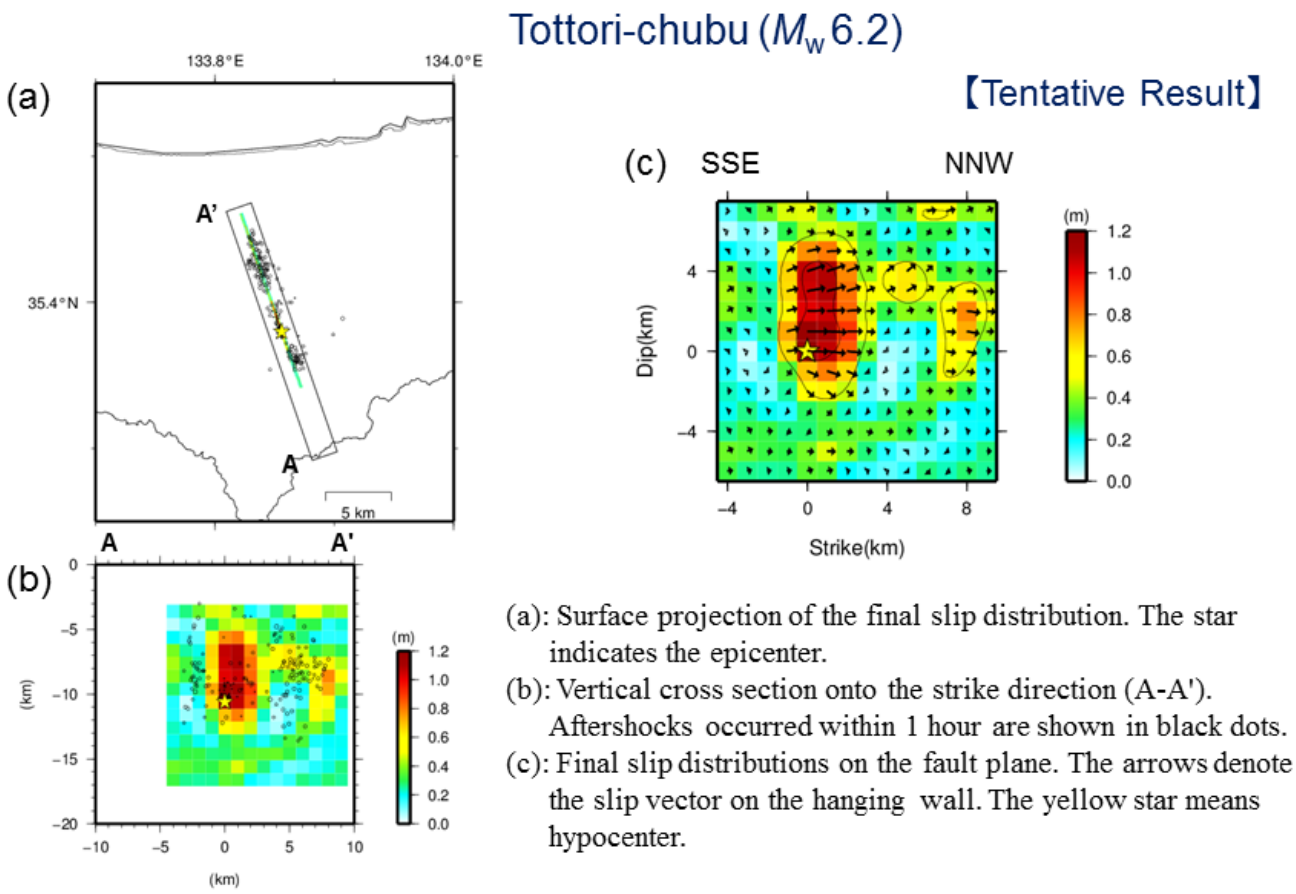

(a): Surface projection of the final slip distribution. The star indicates the epicenter.
(b): Vertical cross section onto the strike direction (A-A'). Aftershocks occurred within 1 hour are shown in black dots.
(c): Final slip distributions on the fault plane. The arrows denote the slip vector on the hanging wall. The yellow star means hypocenter.

Source model for the 2016 mid Tottori prefecture earthquake using Empirical Green's function

*Shohei Yoshida[1], Takao Kagawa[1], Tatsuya Noguchi[1]

1. Graduate School of Engineering, Tottori University

An earthquake of Mw6.2 occurred in the mid area of Tottori prefecture in Japan on October 21 2016. Several research institutions set large number seismometers, that obtained strong ground motions in the area. At several observation points recorded JMA seismic intensity of 6 lower, and partial area were suffered serious damages. Therefore we carry out aftershock and Micro-tremor observation to revel causes of the damages. We tried to estimate source model from those information. It is very important to reproduce the strong motion waveform at damage point for understanding reason of the damages and earthquake disaster mitigation in the future.In this study, we estimate source model of composed asperity through forward modeling with empirical green's function method. The target observation points were 8 in total that are maintained by NIED (K-NET, KiK-net) and Tottori prefecture. We selected foreshock event of Mw4.1 at 12:12 on October 21 2016 as an empirical green's function. The position of asperity was referred to previously conducted to heterogeneity slip distribution model, and each source parameters (e.g. rise time, rupture velocity) were determined by try and error. The estimated source model can reproduced the observed strong motion waveform. However, at several points are not sufficiently reproduced. In order to improve reproducibility of observed strong motion, it needs more detailed examination.

Keywords: 2016 mid Tottori prefecture earthquake, Source model, Empirical green's function

Source inversion using empirical Green's functions for the 2016 Tottori earthquake (Mj 6.6)

*Yoshiaki Shiba[1]

1. Central Research Institute of Electric Power Industry

During the 2016 Tottori earthquake on October 21, the peak ground accelerations at K-NET Kurayoshi (TTR005) reached 1381 gal. Since the station is located just above faulting area, spatial and temporal source rupture process would strongly affect the strong motions at TTR005. The response spectrum calculated from the strong motion record of TTR005 shows relatively large amplitude in the frequency range higher than 1 Hz, therefore the analysis of source process should take into account such higher frequency ground motions. In this study the inversion method using empirical Green's functions is adopted for the source modeling of the Tottori earthquake in order to evaluate broadband ground motions.

From the aftershock distribution and CMT solution of the main shock estimated by F-net, we assumed the left-lateral fault plane model with the strike in the NS direction and the nearly vertical dip angle. Observed records from the aftershocks of Mj 4.0 occurring just beneath TTR005 were used for the empirical Green's functions. Velocity motions of two horizontal components for KiK-net subsurface stations and near-source K-NET stations are used for the source inversion in the frequency range from 0.2 to 2 Hz. Once the moment density distribution on the fault plane is estimated, the effective stress is searched with moment density simultaneously by using the histogram of estimated model parameters as prior probability distribution for the inversion procedure.

The obtained source model indicates large slips mainly in the shallow area around the hypocenter and secondary large slips just beneath TTR005 station, which is located about 5 km north of the epicenter. Estimated rise time on the fault plane is as short as 1.6 seconds at maximum. From the slip distribution of the main shock, it suggests that strong motions at TTR005 area radiated from these two SMGAs sequentially. In case of inversion analysis without records of TTR005, the secondary large slip does not vanish in the estimated source model.

The simultaneous inversion of effective stress and moment density revealed that the shallow large slip area beneath TTR005 shows relatively small effective stress, while the asperity near the hypocenter implies also large effective stress. It is considered to be consistent with the empirical relation that shallow SMGA tends to show small stress drop compared to deep SMGA.

Keywords: 2016 Tottori earthquake, source model, empirical Green's function, strong ground motion

Source imaging of the 2016 Kumamoto earthquake by back-projection of near-filed P wave records.

*Mitsutaka Oshima[1]

1. Shimizu corporation

A series of strong ground motion caused by 2016 Kumamoto earthquake (hereafter, Kumamoto earthquake) devastated the areas along Futagawa-Hinagu fault zone and strong ground shake with Japan Meteorological Agency Seismic Intensity Scale 7 was observed twice for the first time in domestic history of earthquake observation.
Several studies on the spatio-temporal slip distributions have been reported based on waveform inversion pointing out heterogeneity of rupture process, such as depth dependency of slip velocity function.
The direction and the speed at which fault rupture proceeds, as is well known, controls major feature of ground motion around the causal faults. About the Kumamoto earthquake, spatio-temporal distribution of seismic wave emission has been studied by several researchers and those results show that the rupture propagated across fault planes with different strike and dip. Abrupt acceleration of rupture speed has also reported and these fact features the heterogeneity of fault rupturing occurred during the Kumamoto earthquake.
Although rupture heterogeneity strongly affects strong ground motion, it has been only partially taken into account in the current framework of strong ground motion prediction. Slip velocity function and rupture velocity variable on the fault planes are expected to be take into consideration in the future strong ground motion evaluation, and actually, some attempts to incorporate such heterogeneity in fault models for ground motion prediction are under way in the world. Hence, accumulation of information on fault rupturing process is essential to constitute a heterogeneous source model. In this study, I applied back-projection technique to reveal the time history of seismic wave emission during the Kumamoto earthquake.
Strong motion records recorded at 27 KiK-net and K-NET stations within 100km hyopocentral distance were used. Waveforms were rotated according to seismometer orientation and offsets were removed. Then the records were integrated into velocity by lattice filter of Kinoshita(1986). Traveltime data were processed in the similar way as Takenaka and Yamamoto(2004) to obtain seismic emission image with more precision in relative location. Further correction for travel time data was made by using the difference between observed and calculated traveltime from the hypocenter.
The back-projection technique used in this study is similar to that by Kao and Shan(2004), and Ishii et al.(2005). Waveforms were stacked with a combination of Hann window and N-th root stacking. The fault plane was determined from distribution of aftershocks although no assumption for fault plane is necessary in back-projection method.
As a result, some image of rupture propagation from Takano-Shirahata segment of the Hinagu fault zone to Futagawa segment of the Futagawa fault zone was obtained, where the strike and the dip of those two fault planes are different. The rupture rapidly increased its seismic wave emission while it’s moving toward northeast. However, both accuracy and resolution of the present results still leave plenty of scope for improvement. In the future study, I am planning to scrutinize data and data processing techniques, such as traveltime data and waveform stacking methods to get more exact and high-resolution image of the source process.

Acknowledgement: I would like to express my gratitude to NIED for providing me with KiK-net and K-NET data.

Keywords: back-projection , source imaging, Kumamoto earthquake

Study on spectral decay characteristics in high frequency range of observed records during The 2016 Kumamoto Earthquakes

*Masato Tsurugi[1], Takao Kagawa[2], Kojiro Irikura[3]

1. Geo-Research Institute, 2. Tottori University, 3. Aichi Institute of Technology

Spectral decay characteristics of ground motions for the 2016 Kumamoto earthquakes are examined. In this study, spectral decay characteristics in high frequency range are evaluated by two approaches. One is f_{max} filter, the other is spectral decay parameter, κ (Kappa).
In result, f_{max}'s of large earthquakes are estimated to be 7Hz to 10Hz and the larger earthquakes are, the smaller f_{max}'s tend to be. The power coefficient of f_{max} filter, s, of largest foreshock and mainshock of the 2016 Kumamoto Earthquake are larger than those of large earthquakes occurred in other region. From this result, a region dependency of spectral decay characteristic is suggested.
κ's of large earthquakes are estimated to be 0.0466 to 0.0482. There are positive correlation between s as power coefficient of high-frequency decay of f_{max} filter and κ as spectral decay parameter and between f_{max} for the f_{max} filter and f_E for parameter κ. f_E is a frequency at which spectrum starts to decrease on log-linear scale. f_E is a very important parameter for strong ground motion prediction, however f_E has not been examined carefully enough in previous κ studies. It is confirmed that evaluated high frequency characteristics by f_{max} filter and those from spectral decay parameter, κ agree well with each other.

Keywords: The 2016 Kumamoto Earthquakes, Spectral decay characteristics, fmax filter, Kappa

Appropriate Q value model in the Kanto region for simulating long-period ground motion

*Takahiro Maeda[1], Nobuyuki Morikawa[1], Asako Iwaki[1], Hiroyuki Fujiwara[1]

1. National Research Institute for Earth Science and Disaster Resilience

In this study, we investigate an appropriate Q-value model in the Kanto region for evaluating the ground motion on the engineering bedrock that has S-wave velocity of about 350 m/s by comparing the simulated ground motion with the observed data.

We use the ground-motion simulator (GMS; Aoi et al., 2004) which is a practical tool for seismic wave propagation simulation based on 3D finite difference method with fourth order of accuracy in space and second order in time using discontinuous grids. In the GMS, a method to introduce an anelastic attenuation effect easily in the time domain proposed by Graves (1996) is adopted. In this method, an attenuation function for S wave, $a(x,y,z)=\exp(-\pi f_0 \Delta t/Q_S(x,y,z))$, where Q_S is the spatially variable Q value for S wave, f_0 is the reference frequency and Δt is a time interval, is multiplied to the velocity and stress fields at each time step to introduce the anelastic attenuation. Since the Graves' s method is widely used, we examine the suitable Q value for applying the Graves' s method.

The velocity structure model used in this study is a shallow-deep integrated velocity structure model constructed in the Kanto region by integrating shallow structure (Vs < 350m/s) and deep structure. This velocity structure model was verified by comparing the observed and simulated ground motions of M4-5 earthquakes (Maeda et al., 2015, SSJ). In this verification, emphasis is placed on the reproduction of the periodic characteristics of the ground motion caused by the subsurface structure, and thus a goodness of fit between the observed and simulated ground motion is evaluated in the periodic domain using the Fourier spectral ratio. In the evaluation of the degree of fit, referring to the criteria of the SCEC broadband platform validation exercise (Goulet et al., 2015; Dreger et al., 2015), it is judged that the goodness of fit is high when the spectral ratio is within the range of 1/1.4 to 1.4, while the fit is low when the ratio is 1/2 or less, or 2 or more. Averages of spectral ratios calculated from all the data of 5 earthquakes recorded at 197 observation points and averaged spectral ratio at each observation point are within the range of 1/1.4 to 1.4 in the period range of 2 to 10 second. The verification shows that the shallow-deep integrated velocity structure model has been confirmed to be a highly descriptive model of the observed data. However, the period dependence that the amplitude of the simulated spectra is larger than that of the observed one at the shorter period range is recognized, suggesting the possibility of improving the goodness of fit by changing Q value. Therefore, we set up several Q value models to investigate whether the goodness of fit is improved.

In past studies, the Q value model in which $Q_0(=Q_S)$ is proportional to S-wave velocity as $Q_0=\alpha V_S$ (the unit of V_S is m/s) is adopted. For example, $\alpha=0.2$ is assumed in the Japan Integrated Velocity Structure Model (Koketsu et al., 2008; Earthquake Research Committee, 2012). In this study, we use the Q value model proportional to the S-wave velocity and assume that $\alpha=0.1$, 0.2, 0.5, 1.0, and the reference period ($T_0=1/f_0$) is 3 s. Among them, the setting of $\alpha=0.2$ is the same setting as the above verification. Qualitatively, as α decreases, the effect of attenuation due to Q value increases, so the amplitude of the simulated spectra decreases. As a result of investigating the change of averaged spectral ratio of all the data, the change in α is affecting spectral ratio particularly at the shorter period range and thus it is confirmed that the goodness of fit is improve by setting $\alpha=0.1$. In addition, the average value of the

spectral ratio for each observation point also tended to be close to 1 when $\alpha = 0.1$.
Furthermore, in addition to the study in the frequency domain above, we also study in the time domain focusing on the duration. Comparing the envelope shapes of the velocity waveforms of observed and simulated records, it is possible to roughly explain the decay characteristics of observed data using the Q value model set in this study. However, since the data length of the observed data is not enough, consideration of an appropriate α in the time domain is a future task.

Acknowledgement This study was supported by “Support Program for Long-Period Ground Motion Hazard Maps” of the Ministry of Education, Culture, Sports, Science and Technology (MEXT).

Keywords: Q model, shallow-deep integrated velocity structure model, long-period ground motion, GMS

Studies on Qs at the northern part of Kyushu district in Japan.

*kenichi Nakano[1], Shigeki Sakai[1]

1. HAZAMA ANDO CORPORATION

We have reported the variability of Qs in southern part of the Kyushu district, in the previous paper. In that paper, we used seismograms, which are from the M4-5 small-adequate scale earthquake observed by K-NET and KiK-net operated by the National Research Institute for Earth Science and Disaster Resilience, for evaluating the Qs in those areas. As a result, it showed that the average apparent Qs of the line, connecting the seismic source location to the earthquake catalog of JMA and the observation point, changes significantly, depending on regions (route combination of propagations). This suggests that it is necessary to use an appropriate Qs model in the target area, for strong ground motion simulations based on the statistical Green's function method or the like, for example.

In this paper, we evaluate the Qs for the northern part of Kyushu, as the damping properties, using the twofold spectral ratio method. First, the northern part of the Kyushu district was divided into “Region A” and “Region B” as shown by the light orange hatch in Fig. 1. In addition, the area in the southwestern part of the Kyushu district was indicated as “Region C” with a light blue hatch (we had already reported the Qs to the area in our previous paper). In the figure, epicenter distributions of the events occurred after the 2016 Kumamoto earthquake (April 14, 2016 to April 30, 2016) are showed as hollow circles, and red triangles also indicate seismic observation points in NET & KiK-net. The location of the epicenter is referenced to the JMA earthquake catalog. In the area shown in the figure, the evaluation of Qs was carried out in an area having a planar spread (Area), and as a propagation route (Line) respectively. However, since it was difficult to set the Area for “Region B”, only evaluation in Line was carried out. The name of each analysis case was written like “Region A-Area” or “Region A-Line”.

The results are shown in Fig. 2. As can be seen from this figure, it is clear that different Qs models are evaluated in Area-case and Line-case at each region, and also, Qs models are very similar in “Region A” and “Region C”. On the other hand, “Region B” is very different from other regions, Qs = 20*f^1.0 is evaluated. This model agrees to the Qs estimated by Izutani (2000), he assumes the propagation path as just under Mt. Krishima. The propagation path of “Region B” in this study is just under Mt. Aso because we want to secure the propagation distance. Lin et al. (2016) reports the existence of magma chamber from 5km to 10km depth under Mt. Aso. These facts suggest us the possibility that Qs model of “Region B” follows the same theory they pointed out. The Qs models in other regions are harmonious with the one estimated by Uchiyama and Yamamoto (2016). However, it is different from the value evaluated by Nakano et al. (2015). It seems to be due to the fact that the conditions, for example hypocentral distance, are different, and the area to be analyzed is also greatly different. In fact, we also conducted generalized spectral inversion analysis, under conditions tailored to Uchiyama and Yamamoto (2016) and Sato (2016), and confirmed that the Qs model estimated by the analysis is the same as the one proposed by Uchiyama and Yamamoto (2016).

Since our results include only small number of earthquakes and the area to be analyzed, we have to continue the investigation for studying attenuation properties to perform the analysis, considering the variability of earthquakes and propagation path. As our future tasks, we plan to develop a method for evaluating complex damping structures in order to improve the accuracy of strong ground motion prediction.

Acknowledgements: We used the strong motion records provided by National Research Institute for Earth Science and Disaster Resilience (NIED) in this study. We gratefully appreciated it.

Keywords: Qs, Propagation pass, Twofold spectral ratio method

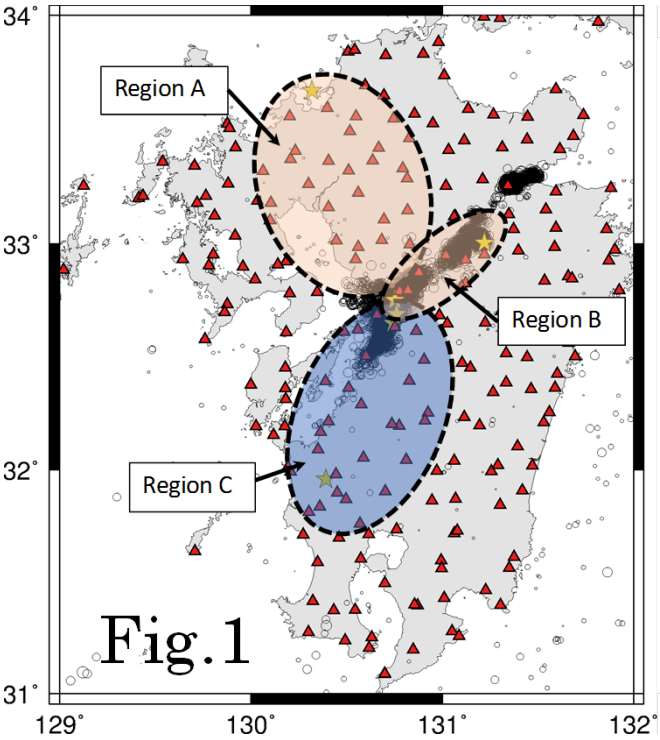

Fig.1

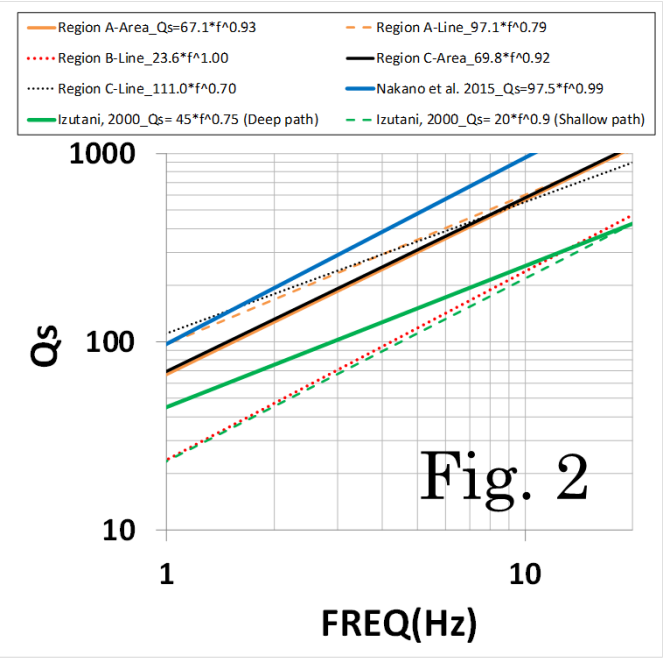

Fig. 2

A New Multidimensional Attenuation Relationship for Instrumental Seismic Intensity

*Hiroto Tanaka[1], Ritsuko S. Matsu'ura[2], Mitsuko Furumura[2], Tsutomu Takahama[1]

1. Kozo Keikaku Engineering Inc., 2. Earthquake Research Center, Association for the Development of Earthquake Prediction

Matsu’ura et al. (2011) and Noda et al. (2016) proposed a multidimensional attenuation relationship of the velocity response spectra for wide range of distance and period, by using the attenuation term proportional to depth of subducting slab. In this study we propose an attenuation relationship for JMA seismic intensity in the same way.
We constructed database using strong-motion records from K-NET and KiK-net, which have peak ground velocity of 0.1 cm/s or more. The database was divided into three groups by seismic source types of Inter-Plate, Intra-Plate, and Very Shallow (VS) earthquakes in Japan. Inter- and Intra-Plate earthquakes occurred on and in subducting Pacific plate. We used the same formula of attenuation relationship as that of velocity response spectra after comparing trends of seismic attenuation between the velocity response and instrumental seismic intensity.

$$INT = Ac + Aw \cdot Mw - b \cdot \Delta - \beta \cdot \log(\Delta) - d \cdot \min(\delta, 250) \pm \sigma$$

where INT is instrumental seismic intensity, Mw is moment magnitude, Δ is hypocentral distance (km), and δ is depth of upper boundary of the Pacific plate. Ac, Aw, b, β and d are regression coefficients, and σ is standard deviation. For earthquakes with Mw > 7.5, we adopted Δ that is closest distance to the fault rupture. We set the upper limit of δ at around 250 km depth, and it improved the consistency with observation. The coefficient β in the attenuation term which is proportional to $\log(\Delta)$ is often fixed around 2 in other previous studies of attenuation relationship for INT, but in this study we estimated β by regression analysis. The final combination of regression coefficients was determined by AIC, because the optimal combination depends on the seismic source type.
For Inter-Plate, the combination of coefficients Ac, Aw, b, β and d got an optimal solution. The standard deviation in the case using the combination was 0.643 and the AIC was also superior, whereas that using conventional simple form (combination of Ac, Aw, b, β) was 0.691. For Intra-Plate, the combination of coefficients Ac, Aw, β and d got an optimal solution. The attenuation relationship of Intra-Plate could explain the observation by the attenuation terms of coefficient β and d (without coefficient b) because there was few data at the short distance. The standard deviation in the case using the combination of Ac, Aw, β and d was 0.644, whereas that using combination of Ac, Aw, b and β was 0.751. For the Inter- and Intra-Plate, we found that the attenuation term proportional to δ was an effective term to account for the difference in attenuation such as anomalous seismic intensity distribution. On the other hand, for VS, the term proportional to δ was not effective, and the combination of coefficients Ac, Aw, b, β was got an optimal solution with standard deviation of 0.677.
We compared these results with observed one or other previous studies in order to verify the obtained relationship. In the Inter- and Intra-Plate earthquakes using the attenuation term proportional to the plate depth in this study, the residuals between observed and predicted by this study is smaller than that by other studies over a wide range of distances. On the other hand, in VS earthquakes without attenuation term proportional to plate depth in this study, the seismic intensity predicted by this study and by other studies are in the same range, and the difference of the residuals between the predicted and observed of for each study was small. These suggest that the attenuation term proportional to δ in this study is

effective to explain observed data.
We will perform further study for a correction term of ground amplification to predict seismic intensity more accurately at arbitrary sites.This study was conducted as an entrusted research from Ministry of Education, Culture, Sports, Science and Technology. We used strong-motion records from NIED K-NET and KiK-net.

Keywords: Ground Motion Prediction Equation (GMPE), Attenuation term proportional to plate depth, Selection by AIC

Type	*Ac*	*Aw*	*b*	β	*d*	σ
VS	2.096	0.962	0.00287	2.409	-	0.677
Inter-Plate	4.726	0.674	0.00171	2.416	0.00527	0.643
Intra-Plate	2.509	1.444	-	3.576	0.00883	0.644

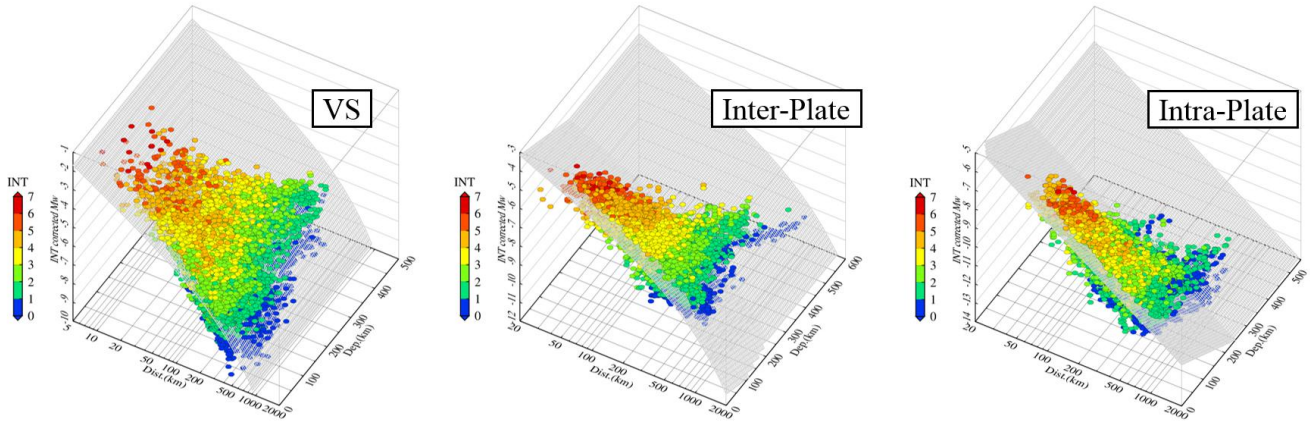

Seismic activity modeling of earthquakes occurred on inland active faults with smaller magnitude than assumed characteristic event for probabilistic seismic hazard

*Jun'ichi Miyakoshi[1], Takeshi Morii[2], Mitsutaka Oshima[2], Nobuyuki Morikawa[3], Hiroyuki Fujiwara[3]

1. Ohsaki Research Institute, Inc., 2. Shimizu Corporation, 3. National Research Institute for Earth Science and Disaster Resilience

In this study, we model seismic activity of earthquakes occurred on inland active faults with smaller magnitude than assumed characteristic event for probabilistic seismic hazard. Examples of these earthquakes are northern Nagano prefecture earthquake in 2014 (M6.7) and Kumamoto earthquake in 2016 (M6.4).
For a part of these earthquakes, probabilistic seismic hazard map by the Headquarters for Earthquake Research Promotion (HERP) are modeled seismic activity of earthquakes that does not show signs on the surface. We consider three new models for these earthquakes referred to the model of HERP. In the model of HERP, the upper limit of magnitude is assumed characteristic event on active fault or 7.4, the lower limit of magnitude is 6.8, and the mean recurrence interval is twice the interval of the active fault. In Model 1, the lower limit of magnitude is 6.5 among the model of HERP. In Model 2, the mean recurrence interval is equal to the interval of the active fault among the model of HERP. Model 3 is combined Model 1 and Model 2.
We calculate probabilistic seismic hazard map based on three new models. As a result, the seismic hazard of Model 3 is the largest, and the seismic hazards of Model 1 and Model 2 are comparable.

Seismic intensity distribution and validation of the source location and the magnitude of the 1914 Sakurajima earthquake

*Reiji Kobayashi[1], Yukina Furuya[2,3], Hiroki Kuwahara[2]

1. Graduate School of Science and Engineering, Kagoshima University, 2. Faculty of Science, Kagoshima University, 3. Grand Lacere Kagoshima

The 1914 Sakurajima earthquake (M 7.1) occurred about eight hours after the eruption of Sakurajima. The seismic intensity distribution in Kagoshima city is estimated from the damaged data of houses and stone block walls (Imamura, 1920). The intensity data used in Imamura (1920) is originally defined in his study and cannot be directly compared to the present seismic intensity scale in Japan defined by the Japan Meteorological Agency (JMA) in 1996. Takemura and Toraya (2015) proposed a conversion procedure from damage data of houses to the present seismic intensity scale for the 1944 Tonankai earthquake.

The seismic intensity distribution in Kyushu Island has also compiled by Imamura (1920) and its isoseismal maps were drawn by Imamura (1920) and Omori (1922). The intensity data can be compared to the present seismic intensity in JMA scale, because the present seismic intensity scale was revised several times from that used for the isoseimal map for the Kyushu Island in Imamura (1920).

In this study, we convert from the damage data of houses in Kagoshima city (Imamura, 1920) to the present seismic intensity in the JMA scale. We also review the seismic intensity distribution in Kyushu Island. Then we verify the source location and magnitude using an attenuation relation of seismic intensity for Japan presented by Morikawa et al. (2010).

Imamura (1920) presents the total number of households but does not present the total number of houses. The sum of the completely destroyed, half destroyed, and partially damaged houses are larger than the number of household in a town, Shiomi-cho. We adopt two assumptions for the total number of houses. One is that the total number of houses in each town is equal to that of householders in it. The other is that the ratio of total number of houses to that of householders in each town is equal to the ratio in Shiomi-cho. The true value may be between those inferred from the two assumptions. The distribution of the present seismic intensity scale adopting the former assumption shows that the maximum intensity is 6 Upper, and that adopting the later assumption is that the maximum intensity is 6 Lower. The maximum difference between the intensities at a same place adopting the two assumptions is one grade.

We also plot the seismic intensities in Kyushu Island to review the isoseismal maps of Imamura (1920) and Omori (1922). The isoseismal contours of both papers are inconsistent to the intensity data at several observation points. It is difficult to draw the isoseismal contours being consistent with the seismic intensity data.

We verify the source location and magnitude of the 1914 earthquake. The source fault of the 1914 Sakurajima earthquake has not been investigated in previous studies. Kagoshima Prefecture assumes a source fault for the same type of an earthquake as the 1914 Sakurajima earthquake to predict the strong ground motions for disaster prevention. The seismic intensities predicted by the attenuation relation with Mw 7.1 are much higher than the observed ones in Kagoshima city. When the magnitude is fixed at Mw

7.1, the source fault location should be moved at least 50 km further from the assumed fault. If the source fault location is fixed, the magnitude should be 5.6. The comparison of the predicted seismic intensity to the observed ones in Kyushu Island shows that Mw 7.1 is too large.

Keywords: The 1914 Sakurajima earthquake, seismic intensity, magnitude

Seismic Intensity Distribution of the 1889 Meiji Kumamoto Earthquake

Noriko Niida[2], *Yoshiko Yamanaka[1]

1. Graduate School of Encironmental Studies, University of NAGOYA, 2. Department of Earth & Planetary Sciences, University of NAGOYA

We investigated historical earthquakes in the Kumamoto Prefecture. We collected historical earthquake information in the history books of the prefecture or the municipalities, historical newspapers, and Official Gazette.
On July 28th 1889 (Meiji 22), the earthquake (M=6.3) occurred at the west of Kumamoto city. Damage statistics on each municipality are reported in Official Gazette. Using seismic damage of house, bridge and crack in the ground, we estimated seismic intensity based on the relationship between seismic intensity and seismic damages proposed by Usami(2016) and obtained the distribution of seismic intensity of this event. The obtained seismic intensity map was compared with the site amplification factor data by National Research Institute for Earth Science and Disaster Resilience (NIED). It seems that the region which have larger site amplification factor tends to become higher seismic intensity.
Takemura(2016) estimated seismic intensity distribution from the collapsed houses reported by Imamura(1920) . His seismic intensity distribution almost resembles one in this study. In some area, seismic intensity of this study came to have a bigger 2-3 rank as his result. Because we estimated seismic intensity from damage of bridges and crack in the ground as well as the damage of the house, our estimated seismic intensities become a little bigger. Houses in the Meiji period were generally located on relatively strong ground which have small value of amplification factor. On the other hand, bridges often stand on the weak ground.
We concluded that seismic intensity determined from damage of houses sometimes becomes smaller than that from damage of other structures.

Keywords: the 1889 Meiji Kumamoto Earthquake, Seismic Intensity Distribution

Simulation of Long-Period Ground Motion in Damaged Areas during the 2016 Kumamoto Earthquake

*Kengo Muroi[1], Hiroaki Yamanaka[1], Kosuke Chimoto[1], Seiji Tsuno[2], Hiroe Miyake[3], Nobuyuki Yamada[4]

1. Tokyo Institute of Technology Department of Environmental Science and Technology, 2. Railway Technical Research Institute, 3. Earthquake Research Institute, University of Tokyo, 4. University of Teacher Education Fukuoka

The 2016 Kumamoto earthquake contains a foreshock with a Mj of 6.5 on April 14 and the main shock with a Mj of 7.3 on April 16. The earthquakes generated ground motions with a seismic intensity of 7 on the Japan Meteorological Agency twice in Mashiki,Kumamoto,Japan and many wooden houses were collapsed. In this study we conducted a simulation of strong ground motion during aftershocks of the 2016 Kumamoto earthquake, using subsurface structural model by Headquarters for Earthquake Research Promotion and GMS, and evaluated earthquake ground motion in the damaged areas. We assumed homogeneous fault model from a group of point sources. We used the aftershock with a Mj of 5.5 and a depth of 10km on April 19. First, we compare the waveform of rock site (KMM014). The calculated waveform has similar characteristics of the observed waveforms. Then, we compare observed ground motion records by Yamanaka et al. (2016) in the damaged areas with the calculated waveforms. The calculated waveforms in the damaged areas have similar characteristics of the observed waveforms which are characterized by long-period S-wave after initial S-wave in about 5 seconds. We also found high correlation between the amplitude of the ground motion and the damages at some observation points.

Keywords: Kumamoto Earthquake, Simulation of ground motion, Strong ground motion

A Study on Characteristics of Long-Period Ground Motion in the Kathmandu Valley during the 2015 Gorkha Nepal earthquake aftershocks

*Michiko Shigefuji[1], Nobuo Takai[2], Subeg Bijukchhen[2], Masayoshi Ichiyanagi[2], Tsutomu Sasatani[2]

1. Kyushu University, 2. Hokkaido University

The Indian Plate underthrusts the Eurasian Plate resulting in occurrence of a number of large earthquakes in the Nepal Himalaya. The Kathmandu Valley is formed by drying of a paleo-lake and consists of thick soft sediment below the center of city. We have installed a strong motion east-west line array observation (four sites; one rock site and three sedimentary sites) in the valley, on 2011, to understand the site effects of the valley. On 25 April 2015, a large M_W 7.8 earthquake occurred along the Himalayan front. The epicenter was near the Gorkha region, 80 km north-west of the Kathmandu Valley, and the rupture propagated eastward from the epicentral region passing through the valley and reached about 80 km north-east of the valley. The aftershock of M_W 6.6 occurred on 25 April 2015 ~80 km northwest of Kathmandu at epicenter near to that of the main shock. The other three large aftershocks were originated ~80 km east of Kathmandu; the aftershock of M_W 6.7 occurred on 26 April 2015 and the aftershocks of M_W 7.3 and M_W 6.3 occurred on 12 May 2015. The ensuing aftershock activities are concentrated in the eastern part of the rupture area. After the mainshock, we installed additional four stations on sedimentary sites on 05 May 2015. We discuss the characteristics of long-period ground motion in the Kathmandu Valley based on these strong motion records from large aftershocks ($M_W > 6$).

The acceleration waveforms at the sedimentary sites are longer and larger than those at the rock site. We checked acceleration Fourier spectra of 40.96 sec of S-wave with rotated acceleration records for each sites and compared between the rock site and other sedimentary sites. In high frequency range (around 0.2 Hz ~), we can observe the strong amplification factor in each site condition. On the other hand, the amplification are extremely small in low frequency (~ around 0.2 Hz) on horizontal components, whereas amplitude are almost same on vertical component. In low frequency range, the spectra have peak in 0.1 ~ 0.2 Hz even in the rock site. Furthermore, the spectral shape on the low frequency range is proportional not to the square but to the cube of frequency. The transition frequency is around 0.2 Hz, but this frequency has small variations by earthquake. Regarding M_W 7.3, M_W 6.3 aftershocks, vertical components semblance analysis show that 0.1 Hz waves are propagated from epicenter with 3 km/sec phase velocity. The particle motion of vertical-radial component shows the retrograde motion which is fundamental Rayleigh wave.

Considering the shape of spectra in low frequency range, we tried to calculate 1-D theoretical waveforms by the discrete wave number method (Takeo, 1985) with 1-D velocity structure (Crust1.0; Laske *et al.*, 2013) and GCMT source mechanism. By this simulation, the surface waves are contained in the analyzed time window; Rayleigh and Love waves which have 0.1 Hz power reached just after direct S-wave initial motion. Therefore, we understood that the shape of the low frequency range are affected by these surface waves.

Spectral ratios of the sedimentary sites to rock site have different dominant frequency (0.2 ~ 0.8 Hz) and amplitude at each sites. These differences of the spectral shape in closed area speculate the complexity

of the basin structure. The predominant frequencies of the spectra could be roughly explained by theoretical response based on 1-D structures made with geological data and gravity anomaly data (Bijukchhen *et al.*, 2016).

During examination of long period motion on large aftershocks, the characteristics are strongly affected by surface wave. We will study the excitation and propagation of surface wave of the Kathmandu basin extensively, try to examine the amplification characteristics quantitatively, and construct the velocity structure of each site in detail.

Keywords: The 2015 Gorkha Nepal earthquake aftershocks, Kathmandu Valley, Long-Period Ground Motion

Observation of microtremors and aftershocks of the 2016 Kumamoto earthquake in the Kumamoto basin

*Kosuke Chimoto[1], Hiroaki Yamanaka[1], Seiji Tsuno[2], Nobuyuki Yamada[3], Hiroe Miyake[4]

1. Tokyo Institute of Technology, 2. Railway Technical Research Institute, 3. University of Teacher Education Fukuoka, 4. The University of Tokyo

We have performed temporary strong motion observation for aftershocks of the 2016 Kumamoto earthquake at the damaged area due to the event (Yamanaka et al. 2016). We have already completed the observation in the town of Mashiki, village of Nishihara, city of Aso and village of Minamiaso, but the observation in the city of Kumamoto is still continued. We here report the strong motion records and microtremor measurements in the Kumamoto basin.

We have started the temporary strong motion observations immediately after the event of 17 April 2017. Several months after the observation, we removed and reinstalled the temporary stations in the city of Kumamoto and we here report the record observed mainly in July 2016. Two temporary stations were installed in Chuo-ward, one in Higashi-ward, three in Minami-ward, and two in Nishi-ward in the city of Kumamoto. The stations installed in Chuo-ward and Nishi-ward is close to the sites where the apartments had severe damage and liquefaction occurred. Less damage was found at the other stations. We used a seismometer JEP-6A3 (Mitutoyo Corp.) which has a sensitivity of 10V/G or 2V/G with a data logger LS7000XT or LS8800 (Hakusan Corp.). Stations continuously record ground motions with 100 Hz sampling and GPS signals were received for time correction.

It is observed 22 aftershocks with Mj 2~4. The strong motion records vary at each station. High frequency motions were observed at the stations located in the northern east of Kumamoto basin and in the Nishi-ward where the apartment was severely damaged. It is observed long period later phases at the stations in Minami-ward. It is also observed in the spectral ratio to the reference station in the northern east of the city of Kumamoto.

We conducted microtremor array measurements at all the temporary stations and estimated the shallow S-wave velocity structure. At any stations, the low velocity layer having a S-wave velocity of about 150m/s was found and its thickness was more than 15m. The thickness was more than 25m at the station in Minami-ward. It was about 2m at the station located in the middle terrace in Chuo-ward. The site response characteristics calculated from the shallow structures have the first dominant period at the period between about 0.5-1.0 seconds. It is more than 1 second at the station close to the coastline in Minami-ward.

This work was partly supported by the Grant-in-Aid for Special Purposes (16H06298: P.I. Hiroshi Shimizu).

Keywords: The 2016 Kumamoto earthquake, Temporary Strong Motion Observation, Aftershocks, Microtremors

Observation of aftershock due to the 2016 mid Tottori prefecture earthquake and microtremor observation in the structural damage area of mid Tottori prefecture, Japan

*Tatsuya Noguchi[1], Takao Kagawa[1], Shohei Yoshida[1], Sho Nakai[1], Hiroshi Ueno[1], Kazu Yoshimi[1], Shoya Arimura[1]

1. Department of Management of Social Systems and Civil Engineering, Civil Engineering Course Graduate School of Engineering, Tottori University

An earthquake (Mj6.6) occurred in central Tottori Prefecture in Japan on October 21, 2016. We conducted aftershock (strong motion) observation at several temporary sites in this area with housing damages. Characteristics of site amplification effect of the temporary sites were understood from analysis of seismic data. Also densely microtremor observations were carried out to estimate the characteristic of ground vibration in the damage area. Microtremor H/V spectra and a distribution of the predominant period were obtained from observation data. In addition, we checked the relationship between site effects and transfer functions of SH-wave, S-wave velocities, H/V of microtremor strong ground motion.

Keywords: 2016 mid Tottori Prefecture earthquake, aftershocks observation, microtremor observation

Site characteristics in Okayama prefecture inferred from strong-motion records of the 2016 Kumamoto earthquake

*Ayumu Uneoka[1], Masanao Komatsu[2], Hiroshi Takenaka[2], Keiichi Nishimura[3]

1. Okayama University, 2. Graduate school of Okayama University, 3. Okayama University of Science

The mainshock of the Kumamoto earthquakes (M_{JMA}7.3) occurred in Kumamoto prefecture, Japan, at 1:25 on 16 April 2016 (JST). The ground motion during this event observed on many stations in Southwest Japan, and several seismic stations in southern Okayama and a part of northern mountain area recorded a seismic intensity of 3 on the JMA scale. Since the azimuths, directions from the source toward the stations, are between 40-50 degrees in Okayama, we regard that the source and the path effects are not different for each station. Therefore, the difference among ground motions observed in Okayama only depends on the site effect under each station. In this study, we analyze strong-motion records in Okayama prefecture and evaluate the site characteristics under their stations. We use strong ground motion records at 113 stations from the networks of K-NET and KiK-net in NIED and seismic intensity meter in Okayama prefecture. We pick P- and S-wave arrivals and identify phases by polarization analysis. Since S-wave durations are for about 11 s from polarization analysis, we calculate Fourier spectra for 10 s after arriving S-wave. Setting on OKYH12 station (Ohara) built on the rock as a reference point, we calculate spectral ratio between another stations and the reference point. Also we compute H/V spectral ratio. Then, we measure primary peak frequency in each spectral ratio. Peak frequencies and shapes of spectral ratio for the reference point correspond to ones of H/V spectral raio in coast area and Hiruzen. However, in another area, primary peak frequencies of H/V are lower than ones of the ratio for reference point. Then, comparing to above peak frequency and site amplification rate in J-SHIS, seismic wave is well amplified under their stations, because 3320112 (Urayasu) and 3358860 (Tsuyama) stations have high site amplifications and low primary peak frequencies. Although 3321430 and 3358860 stations in Hiruzen have high PGA and PGV and low primary peak frequencies, site amplification rates are low. Hence, J-SHIS model cannot describe observed facts in their stations.
Acknowledgment: we used the strong-motions records of NIED and Okayama prefecture.

Keywords: Site characteristics, the 2016 Kumamoto earthquake, H/V spectral ratio

Estimation for site amplification characteristics from spectral inversion of ground motion records in Northern Nagano area

*kawai ryouta[1], Hiroaki Yamanaka[1], Kosuke Chimoto[1], Seiji Tsuno[2]

1. institute titech of tokyo, 2. Railway Technical Research Institute

The 2014 Northern Nagano Earthquake generated the maximum intensity of 6 lower at a strong motion station. The serious damage of this earthquake was characterized by a dense area which is 5km away from an observation station with an intensity of 5 higher. In this study we estimated site amplification characteristics by using ground motion records at strong motion stations and aftershock observation stations by Chimoto et al; (2016) in Northern Nagano area through a spectral inversion technique. The results of Q-value in the propagation path and source characteristics by the spectral inversion technique show similar to those from previous studies. The site amplification in a heavy damaged area show large values in a frequency range of 1.0-3.0[Hz]. A good correlation was found in the relationship between the amplification factors at low frequency and AVS30 from the previous studies, This suggest that the heavy damage is controlled by near-surface layers with low S-wave velocity

Keywords: Spectral inversion technique, Site amplification, 2014 Northern Nagano

A method for setting engineering bedrock using records of miniature array microtremor observation in Kanto Area

*Atsushi Wakai[1], Shigeki Senna[1], Kaoru Jin[1], Ikuo Cho[2], Hisanori Matsuyama[3], Hiroyuki Fujiwara[1]

1. National Research Institute for Earth Science and Disaster Resilience, 2. National Institute of Advanced Industrial Science and Technology, 3. OYO

1. Introduction
In order to estimate damage caused by strong ground motions from a mega-thrust earthquake, it is important to improve broadband ground-motion prediction accuracy in wide area. To realize it, it is one of the important challenges to sophisticate subsurface structure models.
On the purpose of precisely reproducing characteristics of seismic ground motions, we have ever collected as many data as possible obtained by boring surveys and microtremor array surveys, and then have modeled subsurface structure from seismic bedrock to ground surface. At present, we are modeling subsurface structure in Kanto and Tokai area in the project conducted by SIP (Cross-ministerial Strategic Innovation Promotion Program), “reinforcement of resilient disaster prevention and mitigation function” of Council for Science, Technology and innovation.
In this study, we attempt to sophisticate shallow subsurface structure models for Kanto area, including Tokyo, where miniature array microtremor surveys have been conducted from the second half of 2014 to 2016. The method is that initial geological models, which were developed based on boring data and surficial geological informaiton in the past, are improved using S-wave velocity structure estimated from records of miniature array microtremor observations. Especially, with connection between shallow and deep ground in mind, we will focus on boundary surface of velocity layer around engineering bedrock from Vs300 m/s to Vs500 m/s regarded as transitional range between shallow and deep ground.

2. Miniature array microtremor observation
About microtremor observations, array observations were conducted in lowland and plateau of Kanto area. It consists of 4-point miniature array with a radius of 60cm and 3-point irregular array from 3m to 10m on a side. These observations are made on the road and near seismic ground-motion stations such as K-NET and KiK-net. The total number of observation sites has reached about ten thousand, as of February in 2017. In addition, we made an observation for 15 minutes per site at intervals of 1km or 2km using JU210/215 or JU410 which is an all-in-one microtremor observation unit. Sampling frequency was 100Hz or 200Hz.

3. Analysis method and the results on shallow subsurface structure
In this study, we evaluated one-dimensional S-wave velocity structure using shallow subsurface structure survey method based on microtremor observation. The method has been proposed and advanced in recent researches [3-5]. We made an analysis in the following procedure using a microtremor analysis tool such as “BIDO” and “Microtremor Array Tools.”
[1]Auto-analysis and reading of disperse curves and H/V spectral ratios
[2]Extraction of amplification factors such as AVS30
[3]Direct depth transformation of disperse curves [Simple Profiling Method; SPM]
[4]Inversion process such as Simple Inversion Method [SIM]
[5]Joint inversion using H/V spectral ratio and initial velocity structure obtained in 3,4 noted above [Linear Inversion]
[6]Extraction of the depth of top surface in Vs350 m/s and Vs500 m/s layer

One-dimensional S-wave velocity structure and two-dimensional cross-section obtained by analysis mentioned above were, if necessary, modified after comparison with existing initial geological models and investigation. As a result, on the river basin, the models were consistent with S-wave velocity structure models based on boring data [initial geological models]. Besides, three-dimensional structure was revealed on velocity layers around engineering bedrock [Vs300 m/s to Vs500 m/s], which cannot be estimated only through boring data.

4. Summary

In this study, we estimated 1-D S-wave velocity structure and 2-D cross-section based on miniature array microtremor observation records in lowland and plateau of Kanto area. And then, more precisely, we set boundary surface of velocity layers after comparison with existing initial geological models and investigation. This challenge can be a key method about modeling of subsurface structure for seismic ground-motion prediction.

Keywords: engineering bedrock, S-wave velocity structure model, miniature array, microtremor

Modeling of 3D S-wave velocity structure for sedimentary layers in Kanto area, using microtremor array surveys –part 2-

*Kaoru Jin[1], Shigeki Senna[1], Atsushi Wakai[1], Hiroyuki Fujiwara[1]

1. National Research Institude for Earth Science and Disarster Prevention

We have ever engaged in modeling of underground structure from seismic bedrock to ground surface in Kanto area for the purpose of improving accuracy of earthquake ground-motion prediction. In order to advance the underground structure models, microtremor surveys have been conducted at a lot of sites in Kanto plain for these several years. “Senna et.al., 2016” shows that the conventional underground structure models were improved by using records of microtremor array surveys conducted by 2015 and earthquake observations.

In this study, by adding results of microtremor array surveys conducted at about 100 sites in 2016, the underground structure models were improved at the target area in comparison with models constructed in 2015. Above all, velocity layers from Vs500 m/s to Vs900 m/s were modified.

Keywords: microtremor array observation, S-wave velocity structure, Underground structure model

3D velocity structure of Oita prefecture, Kyushu, Japan for strong ground motion simulation

*Masayuki Yoshimi[1], Hisanori Matsuyama[2], Haruhiko Suzuki[2], Atsushi Yatagai[2], Takumi Hayashida[3], Shinichi Matsushima[4], Hiroshi Takenaka[5], Hiroe Miyake[6], Keiji Takemura[7]

1. Geological Survey of Japan, AIST, 2. Oyo Corporation, 3. Building Research Institute, 4. DPRI, Kyoto University, 5. Okayama University, 6. Tokyo University, 7. Kyoto University

For reliable strong ground motion prediction, valid velocity structure is essential. We constructed a 3D velocity structure of Oita prefecture up to engineering bedrock (Vs > 500 m/s) and finer 3d structure for Oita Plain additionally. In this study, we observed, collected, and compiled data obtained from microtremor surveys, ground motion observations, boreholes etc., and constructed velocity structure by modifying published one. Velocity structure up to the engineering bedrock is modified so as to reproduce the observed phase velocity and H/V ratio. Finer structure of the Oita Plain is modeled, as 250m-mesh model, with empirical relation among N-value, lithology, depth and Vs, using borehole data, then validated with the phase velocity data obtained by the dense microtremor array observation (Yoshimi et al., 2016).

This work is supported by the Comprehensive Research on the Beppu-Haneyama Fault Zone funded by the Ministry of Education, Culture, Sports, Science, and Technology (MEXT), Japan.

Keywords: shear wave velocity structure model, ground motion prediction, site amplification, microtremor observation

Evaluation of Three-dimensional Basin Structure Model beneath Beppu bay, Oita Prefecture, using Seismic Interferometry

*Takumi Hayashida[1], Masayuki Yoshimi[2], Masanao Komatsu[3], Hiroshi Takenaka[3]

1. IISEE, Building Research Institute, 2. Geological Survey of Japan, AIST, 3. Graduate School of Natural Science and Technology, Okayama University

A dense seismic array has been deployed since late August 2014 around the Beppu Bay area, Oita prefecture, Japan, to investigate S-wave velocity structure of deep sedimentary basin (Hayashida *et al.*, 2015; Yoshimi and Hayashida, 2017). The array consists of 12 stations with an average spacing of 12 km. Each station consists of a three component broadband seismometer (Nanometrics Trillium compact; 750 V/m/s, T=120 s) in a hole with a 24-bit data logger (Hakusan DATAMARK LS-8800; sampling rate of 100 Hz). We used the continuous ambient noise (microtremor) data of about 20 months (from September 2014 to April 2016) to obtain the ambient noise cross-correlation functions (CCFs) between 66 pairs of stations (6.4 km –65.2 km). The derived nine-component inter-station Green’s functions (ZR, ZT, ZZ, RR, RT, RZ, TR, TT, TZ) from the stacked cross-correlation functions show clear wave-trains corresponding to surface-wave propagation between sensors for station pairs that across shallow-bedrock areas, whereas it is still difficult to visually confirm the distinct wave trains for station pairs that across deep sedimentary basin beneath the Beppu Bay area. At first we investigated the spatial distribution of surface wave group velocities between two stations in different frequencies, by comparing the estimated group velocities from the derived CCFs with the multiple filtering technique (Dziewonski *et al.* 1969) and theoretical ones using an existing velocity structure model (J-SHIS v2). We also simulated theoretical Green’s functions for all stations pairs using the finite difference method (HOT-FDM, Nakamura et al., 2012), using the J-SHIS basin structure with land and seafloor topography and a seawater layer with a grid spacing of 50 m (Okunaka *et al.*, 2016). The estimated values of group velocity indicate smaller group velocities in the Beppu Bay area than those in the surrounding areas in the higher frequency range (0.3 Hz-) and generally show good agreements with theoretical ones. The comparisons between obtained and simulated Green’s functions also generally show good agreements in the areas in the frequency range between 0.1 and 0.5 Hz. On the other hand, the comparisons of group velocities and Green’s functions show systematic differences inside Beppu Bay, indicating S-wave velocity beneath the bay might be slower than those of the existing structure model.

Acknowledgements:
This work is supported by the Comprehensive Research on the Beppu-Haneyama Fault Zone funded by the Ministry of Education, Culture, Sports, Science, and Technology (MEXT), Japan.

Keywords: seismic interferometry, surface wave, group velocity, Green's function, ambient noise, finite difference method

The Estimation of 2D S-wave velocity structure model across the Morimoto-Togashi fault zone through miniature microtremor array analysis

*Nayuta Matsumoto[1], Yoshihiro Hiramatsu[2], Shigeki Senna[3]

1. Graduate School of Natural Science and Technology, Kanazawa University, 2. Institute of Science and Engineering, Kanazawa University, 3. National Research Institute for Earth Science and Disaster Resilience

Around the Noto peninsula, ENE-WSW or NE-SW striking reverse faults developed under the E-W compression stress in Quaternary (Okamura, 2007). It is important to reveal the subsurface structures of the faults, which have formed the topography of this region, to understand the geotectonic history of this area.
The object of our study is to reveal subsurface structures of the Morimoto-Togashi fault zone, which is located in southern part of the peninsula. The probability of a large earthquake occurring within the next 30 years is high, 2-8%, and the fault passes the city center of Kanazawa. Therefore, this study is also useful for the disaster prevention. A seismic reflection survey around Togiya, the north part of the Morimoto fault, suggests that the fault structure is an east dipping reverse fault with 40-60 degree, (AIST, 2008). However, the details of the subsurface structures are still unknown. Additionally, the gravity anomaly analysis cannot detect the structural boundary along the fault. In this study, we conduct miniature array analysis (Cho et al., 2013) using miniature arrays with a radius of 0.6 m and irregular-shaped arrays with a radius of 5-15 m. Sampling frequency is 200 Hz and the observation duration is around 15 minutes. Seismometers used for the observation are JU410 manufactured by Hakusan Corporation. We set 11 lines across the fault zone. The intervals of the observation points are 100-200 m. We analyze data with the software BIDO and infer the two-dimensional S-wave velocity sections. The software BIDO combines a simple profiling method (e.g., Heukelom and Foster, 1960), where an S-wave velocity structure is calculated directly from a dispersion curve, and a simplified inversion method (Pelekis and Athanasopoulos, 2011) to estimate the S-wave velocity structure. Around Togiya where the seismic reflection survey was held, the obtained S-wave velocity section shows a discontinuous structure of bedrock (Vs=500 m/s) on the 100 m east side of the surface fault trace. This discontinuity infers the east dipping structure with a high angle, corresponding to the faulting type of the fault.

Keywords: microtremor, miniature array, irregular-shaped array, velocity structure, active fault

Density Structure Model Estimated from Gravity Survey around Mashiki damaged by 2016 Kumamoto Earthquake

Shun Araki[2], Tatsuya Noguchi[3], Masao Komazawa[4], Shoya Arimura[3], Mitsuhiro Tamura[3], Kei Nakayama[3], *Hitoshi Morikawa[1], Takashi Miyamoto[5], Kahori Iiyama[1], Yoshiya Hata[6], Masayuki Yoshimi[7], Takao Kagawa[3], Hiroyuki Goto[8]

1. Department of Urban Design and Built Environemt, Tokyo Institute of Technology, 2. Department of Civil and Environmental Engineering, Tokyo Institute of Technology, 3. Department of Management Social Systems and Civil Engineering, Tottori University, 4. Oyo Corporation, 5. Department of Civil Engineering, Yamanashi Univsersity, 6. Division of Global Architecture, Osaka University, 7. Geological Survey of Japan, AIST, 8. Disaster Prevention Research Institute, Kyoto University

Gravity survey has been carried out around downtown of Mashiki, Kumamoto, Japan, where is severely damaged by 2016 Kumamoto earthquake, from November 28 to December 2, 2016. We applied three LaCoste gravimeters and one Schintrex CG-3M. Closed observations were carried out at more than 300 sites around the central part of Mashiki with about 50-meter intervals. And, more than 150 sites surround the central part with 250- to 500-meter intervals. The observation sites satisfy enough density to discuss density structure shallower than 500-meter depth around central part of Mashiki. After applying some corrections to the observed data, the Bouguer anomaly is calculated under the assumed density of 2.4 g/cm^3. Furthermore, gravity basement is estimated under an assumption of two layered medium with density difference of 0.5 g/cm^3. As a result, a graben runs parallel to the Akitsu river and some isolated small basins are found inside of the graben. The central part of Mashiki is located immediately above of the one of such the small basins. This may suggest that the focusing phenomena of seismic rays.

Keywords: Gravity Survey, Mashiki, Kumamoto, Japan, Density Structure

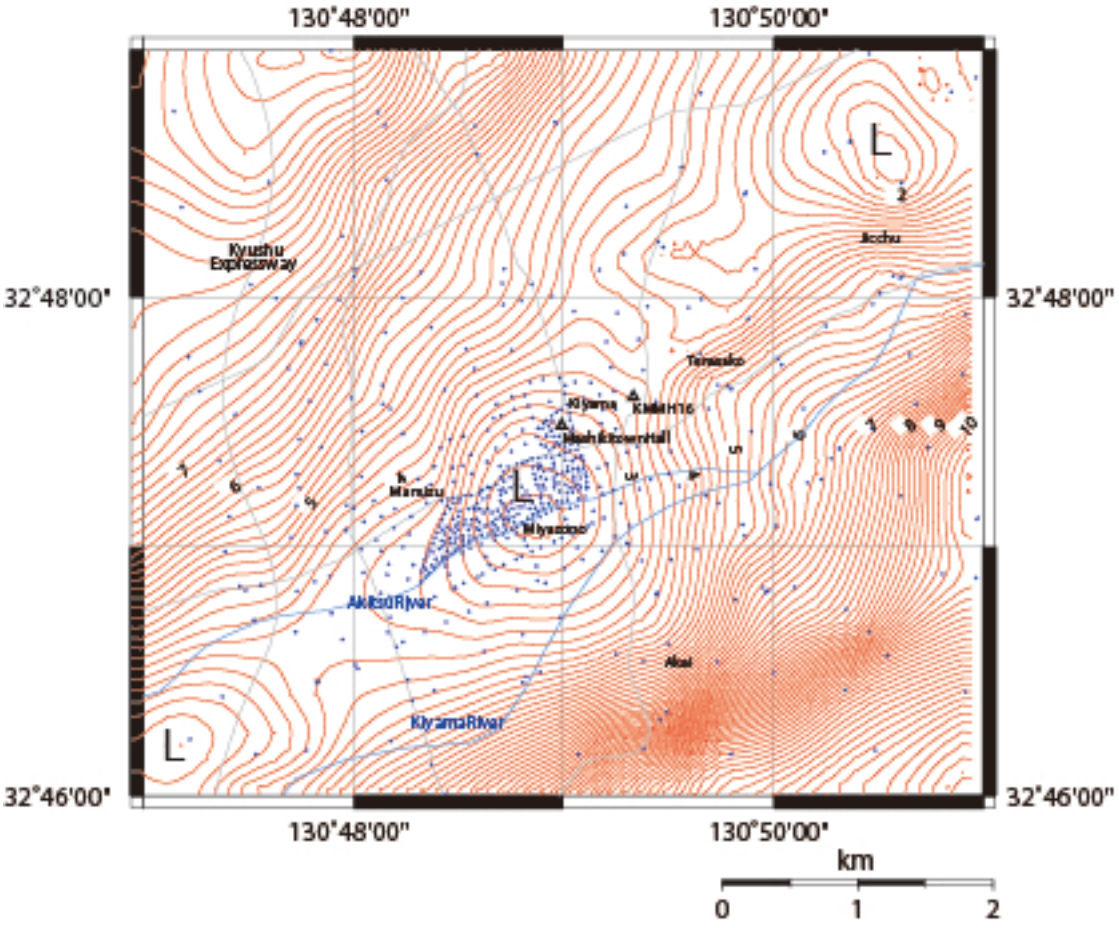

Bouruer anomaly (assumed density = 2.4 g/cm³)

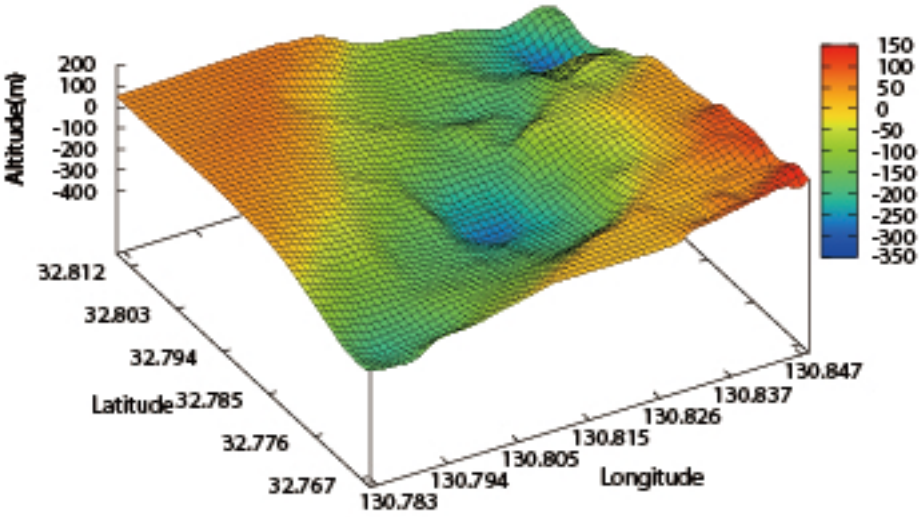

Gravity basement (density difference = 0.5 g/cm³)

Microtremor Array Measurement Survey and Strong Ground Motion Observation Activities of the SATREPS, MarDiM Project, Turkey

*seckin ozgur citak[1], Safa Arslan[2], Ozlem Karagoz[3,7], Kosuke Chimoto[3], Oguz Ozel[2], Hiroaki Yamanaka[3], Bengi Aksahin[2], Ken Hatayama[4], Michihiro Ohori[5], Muneo Hori[6]

1. Japan Agency for Marine-Earth Science and Technology (JAMSTEC), Research and Development Center for Earthquake and Tsunami (CEAT), Yokohama, Japan, 2. Istanbul University, Department of Geophysical Engineering, Istanbul, Turkey, 3. Tokyo Institute of Technology, Dept of Environmental Science and Technology, Yokohama, Japan, 4. National Research Institute of Fire and Disaster, Tokyo, Japan, 5. Fukui University, Research Institute of Nuclear Engineering, Fukui, Japan, 6. University of Tokyo, Earthquake Research Institute, Tokyo, Japan, 7. Canakkale Onsekiz Mart University, Department of Geophysical Engineering, Canakkale, Turkey

Since 1939, devastating earthquakes with magnitude greater than seven ruptured North Anatolian Fault (NAF) westward, starting from 1939 Erzincan (Ms=7.9) at the eastern Turkey and including the latest 1999 Izmit-Golcuk (Ms=7.4) and the Duzce (Ms=7.2) earthquakes in the eastern Marmara region, Turkey. On the other hand, the west of the Sea of Marmara an Mw7.4 earthquake ruptured the NAF’ s Ganos segment in 1912. The only un-ruptured segments of the NAF in the last century are within the Sea of Marmara, and are identified as a "seismic gap" zone that its rupture may cause a devastating earthquake. In order to unravel the seismic risks of the Marmara region a comprehensive multidisciplinary research project The MarDiM project "Earthquake And Tsunami Disaster Mitigation in The Marmara Region and Disaster Education in Turkey", has already been started since 2003. The project is conducted in the framework of “Science and Technology Research Partnership for Sustainable Development (SATREPS)” sponsored by Japan Science and Technology Agency (JST) and Japan International Cooperation Agency (JICA).

One of the main research field of the project is "Seismic characterization and damage prediction" which aims to improve the prediction accuracy of the estimation of the damages induced by strong ground motions and tsunamis based on reliable source parameters, detailed deep and shallow velocity structure and building data. As for detailed deep and shallow velocity structure microtremor array measurement surveys were conducted in Zeytinburnu district of Istanbul, Tekirdag, Canakkale and Edirne provinces at about 140 sites on October 2013, September 2014, 2015 and 2016. Also in September 2014, 11 accelerometer units were installed mainly in public buildings in both Zeytinburnu and Tekirdag area and are currently in operation. Each accelerometer unit compose of a Network Sensor (CV-374A) by Tokyo Sokushin, post processing PC for data storage and power supply unit. The Network Sensor (CV-374A) consist of three servo type accelerometers for two horizontal and one vertical component combined with 24 bit AD converter.

In the presentation current achievements and activities of research group, preliminary results of microtremor array measurement surveys and recorded data by the newly installed stations will be introduced.

Keywords: Satreps, MarDiM project, Seismic observation, Microtremor array measurement

Elaboration of a velocity model of the Bogota basin (Colombia) based on microtremors array and gravity measurements, and strong motion records

*Nelson Pulido[1], Shigeki Senna[1], Hiroaki Yamanaka[2], Helber Garcia[3], Leonardo Quiñones[4], Chimoto Kosuke[2], Cristina Dimaté[4], Mario Leal[5]

1. National Research Institute for Earth Science and Disaster Resilience, 2. Tokyo Institute of Technology, 3. Servicio Geológico Colombiano (Colombian Geological Survey), 4. Universidad Nacional de Colombia (National University of Colombia), 5. Instituto Distrital de Gestión de Riesgos y Cambio Climático (Bogota Agency for Risk Management and Climatic Change)

Bogotá, a megacity with almost 8 million inhabitants is prone to a significant earthquake hazard due to nearby active faults as well as subduction megathrust earthquakes. The city has been severely affected by many historical earthquakes in the last 500 years, reaching MM intensities of 8 or more in Bogotá. The city is also located at a large lacustrine basin composed of extremely soft soils which may strongly amplify the ground shaking from earthquakes. The basin extends approximately 40 km from North to South, is bounded by the Andes range to the East and South, and sharply deepens towards the West of Bogotá. The city has been the subject of multiple microzonations studies which have contributed to gain a good knowledge on the geotechnical zonation of the city and tectonic setting of the region. To improve our knowledge on the seismic risk of the city as one of the topics, we started a 5 years project sponsored by SATREPS (a joint program of JICA and JST), entitled “Application of state of the art technologies to strengthen research and response to seismic, volcanic and tsunami events and enhance risk management in Colombia (2015-2019)”. In this paper we will show our preliminary results for the elaboration of a velocity model of the city. To construct a velocity model of the basin we conducted multi-sized microtremors arrays measurements (radius from 60 cm up to 1000 m) at 41 sites within the city. We calculated dispersion curves and inferred velocity profiles at all the sites. We combine these results with available gravity measurements within the city to obtain the initial velocity model of the basin. We also evaluated site effects in Bogota using records from the Strong Motion Network of Bogota.

Keywords: Site Effects, Strong motion, Bogota basin, microtremors array, gravity

Observation of source rupture directivity and site effect using earthquake early warning systems

*Ting-Yu Hsu[1], Pei-Yang Lin[2], Hung-Wei Chiang[2], Shieh-Kung Huang[2]

1. Taiwan TECH & NCREE, 2. NCREE

The National Center for Research on Earthquake Engineering (NCREE) in Taiwan has developed an on-site Earthquake Early Warning System (NEEWS). The Meinong earthquake with a moment magnitude of 6.53 and a focal depth of 14.6 km occurred on February 5, 2016 in southern Taiwan. It caused 117 deaths, injured 551, caused the collapse of six buildings, and serious damage to 247 buildings. During the Meinong earthquake, the system performance of sixteen NEEWS stations was recorded. The directivity of the earthquake source characteristic and also possibly the site effects were observed in the diagram of the distribution of PGA difference between the predicted PGA and the measured PGA. In addition, based on a preassigned PGA threshold to issue alarms at different stations, no false alarms or missed alarms were issued during the earthquake. About 4 seconds to 33 seconds of lead-time were provided by the NEEWS depending on the epicenter distance.

Keywords: Source Rupture Directivity, Site Effect, On-Site Earthquake Early Warning

Multi-use seismic stations for earthquake early warning

Stephen Kilty[1], Bruce Townsend[1], Geoffrey Bainbridge[1], David Easton[1], *Nahanni McIntosh[1]

1. Nanometrics Seismic Monitoring Solutions

Earthquake Early Warning (EEW) network performance improves with the number and density of sensing stations, quality of the sites and of strong-motion instrumentation, degree of coverage near at-risk populated areas and potential fault zones, and minimizing latency of signal processing and transmission. Seismic research tends to emphasize competing requirements: low-noise sites, high-performance broadband seismic instrumentation, and high-quality signal processing without regard for latency. Recent advances in instrumentation and processing techniques have made feasible the concept of a multi-use seismic station in which strong- and weak-motion seismometry are both cost-effectively served without compromising the performance demands of either.

Our concept for a multi-use seismic station meets the needs of both EEW and high-quality seismic research. One significant enabler is a 6-channel dual-sensor instrument that combines a 120s broadband seismometer and a class A accelerometer in a single ultra-compact sonde suitable for direct burial. Combining two sensors effectively adds broadband capability to a station without increasing the already optimized site footprint, preparation and management costs associated with shallow direct-burial installations. The combined sensors also simplify and speed up installation (for example, the accelerometer provides real-time tilt readings useful to leveling the seismometer). Integration simplifies alignment to north, as there is only one instrument to orient. A dual-use 6-channel digitizer simultaneously provides two sets of independently processed streams from both sensors, one set optimized for low-latency earthquake warning, and the other set for high-quality seismic research purposes.

Such a dual-use seismic station can serve both seismic research and civil warning infrastructure objectives without adding significantly to the cost of a single-use station, while increasing the utility for all users of the station’ s data.

Keywords: earthquake early warning, broadband seismometer, accelerometer, multi-use seismic station

Development of inference methods for rotational motions on ground surface

*koji hada[1], Horike Masanori [2]

1. NEWJEC INC., 2. Hanshin Consultants Co., Ltd.

In this study, we develop two methods for the inference of rotation vector on ground surface, two rocking rotations and a single torsional rotation. The first, termed nth-order elastic method, is based on the elasticity of the ground surface, and the rotation vector is constructed from the first derivative of ground motions which are approximated by nth-order Taylor expansion. Meanwhile, the second, termed rigid method, is based on the rigidity of ground surface and the rotation vectors are directly obtained by the least square method which minimize the sum of the squared difference between recorded differential motions and the equation of the rigid motions. Furthermore, the second is divided into two methods. The one, multi-site rigid method, uses the differential motions at multi sites, while the other, single-site rigid method, uses the differential motions at a single site. Also, we show that the 1st-order elastic method is the same as the rigid method. Appling the nth-order elastic method to microtremor recordings acquired with a small-size dense array, we successfully infer the rotation vector and find the rigid zone with a radius of 5m for the torsional motions. We furthermore obtain the two findings. The first is that the rotation vector can be inferred with a simpler array of a small size and a fewer observation sites. The second is that the root mean squared (RMS) amplitudes of the torsional rotation inferred by the single site rigid method are approximately the same as the RMS amplitudes obtained by the 1st-order elastic method in a zone close to the reference site.

Keywords: Inference methods of rotational motions, Ground surface, Microtremors, Small-size dense array

Study on the backtracking factors of Arias Intensity based on the Ground-motion response spectrum and time-period envelope function parameters

*Liang Xiao[1]

1. Institude of Geophysics, China Earthquake Administration

Arias intensity, as a parameter descripting ground motion amplitude and duration characteristics, has good correlation with earthquake damage such as landslide and sand soil liquefaction. The study on the relationship between the Arias Intensity and the ground-motion response spectrum has important application value in the rapid assessment of earthquake disaster, seismic landslide hazard analysis and so on.
Our previous research found it was difficult to backtrack or reproduce Arias Intensity by using only response spectrum through artificial ground-motion. *Ts*, a critical parameter of the envelope function, defined as the duration of stationary portion of an earthquake record, was found to have great influence on the backtracking results of the artificial Arias Intensity. However, *Ts* could vary a lot due to different rules of definition. Thus, one proper definition of *Ts* is needed to meet the demand for backtracking of Arias Intensity.
In this paper, a set of strong ground-motion records chosen from U.S. PEER NGA database were used as the basic data. The corresponding response spectrum (5% damping ratio) and Arias Intensity was calculated. *Ts* for each record were calculated using several frequently-used definitions. Artificial ground-motion acceleration time periods were generated and were used to reproduce artificial Arias Intensity.
The statistical difference between real values of Arias Intensity and artificial ones were identified. The proper *Ts* was defined as the one that minimizes the difference between the statistical mean of artificial Arias Intensity and the real values. Additional tests showed that backtracking of Arias Intensity could be improved in a statistical sense by using both the response spectrum and proper *Ts* parameter.

Keywords: Arias Intensity, Strong ground-motion, Response spectrum

The detailed explanation of the strong resemblance between Fourier Spectrum and Phase difference Spectrum of the Seismic Wave.(Science of Form)

*Masaru Nishizawa[1]

1. none

1.The phase difference Spectrum and The Phase Wave of the seismic wave.
Fig-(1). Show “The relationship between the phase difference spectrum and the phase wave”. Please refer to reference (3). Find the phase difference Spectrum from the phase wave on the right -hand side, the peak position and added an expanse state of Spectrum are in perfect harmony accord. In short (in other words), in case of the frequency of the phase wave is high, the shape of the normal distribution of the phase difference spectrum is build up sharp. And in the case of large frequency get a flat normal distribution of spectrum. This phenomena stand up all right frequency is high or low. Of course this phenomena is reversible was stated reference (3).
I shall state a next item 2, the seismic wave and this phase wave should be a one-to-one relation. And still more the Fourier spectrum of the seismic wave and the phase difference Spectrum should be a one-to-one relation.
2.The Fourier Spectrum and the normal distribution of seismic wave.
We think that the case of the epicenter length is becoming shorter little by little. The large epicenter length to get along with, the seismic wave energy is dispersed in every direction and still more had died out. As a result, the shape of the Fourier spectrum don’t become a hill shape and happened occasionally a pointed shape. The shorter epicenter length to get along with, the shape of the Fourier spectrum of seismic wave is formed a hill and soon are considered the shape of the normal distribution.
Reference. “Earthquake” written by Seismologist KIYOO Wadachi. The Chuukou Library. (A pocket edition) 1933 and 1993(reprint) p.99
“In the near area to the epicenter, the earthquake have very sharp motion. In many case, intense vertical motion happens in the early shocks of an earthquake. The longer the epicenter length little by little, vibration of seismic wave become slow little by little and becomes superior in a horizontal vibration.”
The shape of this normal distribution has flat hill and besides has large frequency of the peak of the hill. But get shorter little by little, the shape of the normal distribution (or Bell type) becomes sharp and becomes short frequency.
Moreover make the short epicenter length, we shall study the normal distribution theory (Gaussian distribution, Mt.Fuji-type or Bell type) of probability and statics.
In the reference (4), I have explained the KdV equation.(literature (3),(4))
Abstract
1. The shorter epicenter length shorter, the shape of the normal distribution becomes sharp. And this frequency too becomes small. The case of the epicenter length is large, the normal distribution of spectrum of seismic wave was not build up. Only build up a scattered peak.
2. On the case of the phase wave and the phase difference spectrum, the same phenomenon too come into being.
Reference
1. Yorihiko Osaki "Shin Jishindou no Spectrum Kaiseki Nyumon" P78.
2. Masaru NISHIZAWA. (2012): Study of shape of Mountain (Normal Distribution) of Fourier Spectrum of Earthquake Motion. May 20-25, S-SS30-P12(2012, JpGU)

3. Masaru NISHIZAWA. (2012): Handling by Solitary Wave and soliton of Earthquake Motion: October D22-01, 2012, The Seismological Society of Japan.
4. Masaru NISHIZAWA. (2015): Normal Distribution of Seismic Wave Spectrum and Solitary Wave in Water Waves (Science of Form). October 27. S01-P20, 2015, The Seismological Society of Japan.
5. Research Report on the 2011 Great East Japan Earthquake Disaster. NIED, Japan.

* Reference 1: The very excellent and the easy to understand book. I can say with confidence.

Keywords: Fourier Spectrum, Phase difference spectrum, Seismic wave, Phase wave, KdV equation, Solitary wave

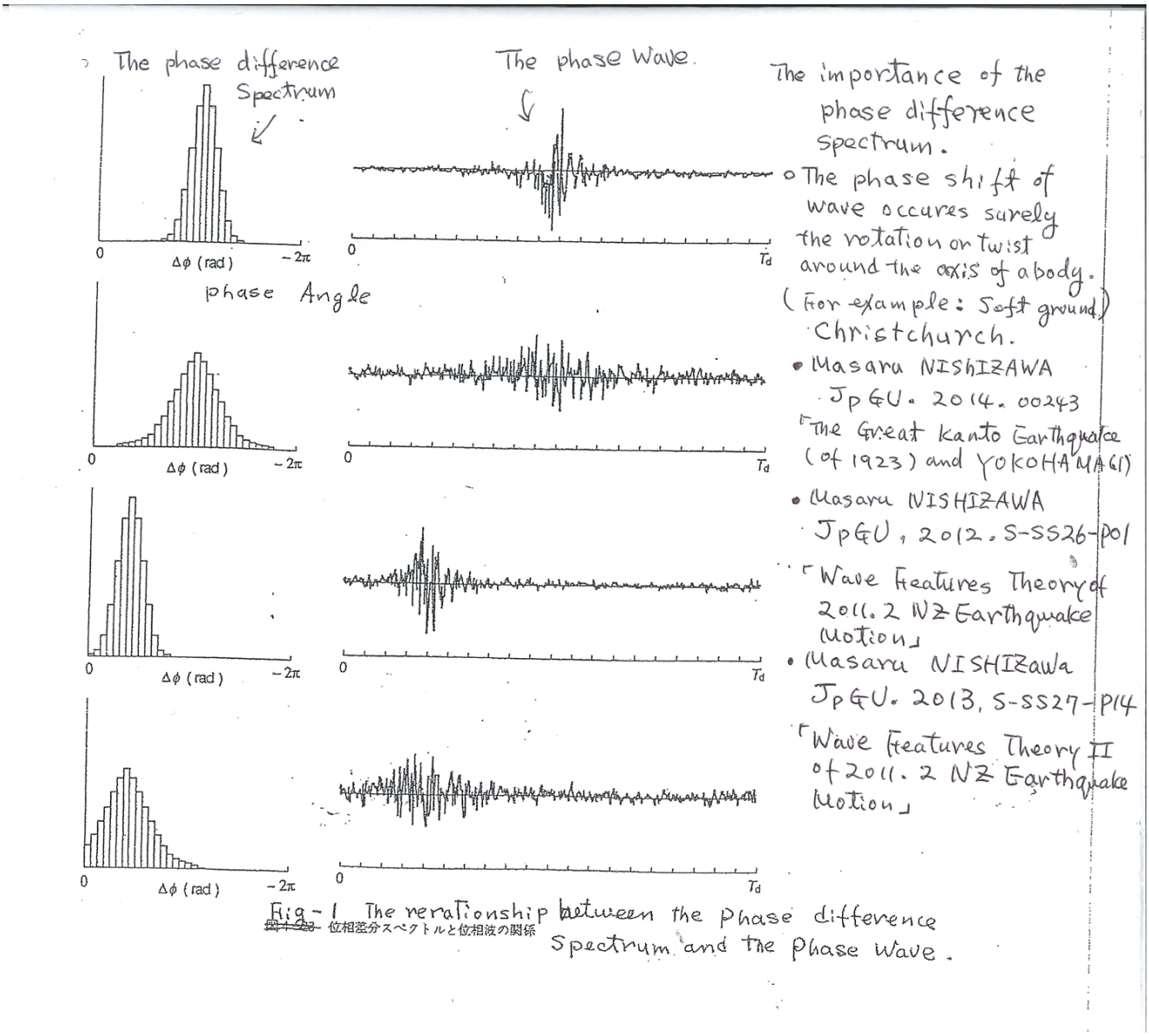

Fig-1 The neralionship between the phase difference Spectrum and the phase wave.
位相差分スペクトルと位相波の関係

